Electrochimica Acta 266 (2018) 364–372

Contents lists available at ScienceDirect

Electrochimica Acta

journal homepage: www.elsevier.com/locate/electacta

Porous reduced graphene oxide modified electrodes for the analysis of protein aggregation. Part 2: Application to the analysis of calcitonin containing pharmaceutical formulation

Alina Vasilescu [a, **], Ran Ye [b], Samia Boulahneche [c, d], Sabrina Lamraoui [c, d], Roxana Jijie [c], Mohamed Salah Medjram [d], Szilveszter Gáspár [a], Santosh K. Singh [e, f], Sreekumar Kurungot [e, f], Sorin Melinte [b], Rabah Boukherroub [c], Sabine Szunerits [c, *]

[a] International Center of Biodynamics, 1B Intrarea Portocalelor, Bucharest, 060101, Romania
[b] Institute of Information and Communication Technologies, Electronics and Applied Mathematics, Université Catholique de Louvain, 1348, Louvain-la-Neuve, Belgium
[c] Univ. Lille, CNRS, Centrale Lille, ISEN, Univ. Valenciennes, UMR 8520-IEMN, F-59000, Lille, France
[d] Laboratoire de Génie Chimique et Environnement de Skikda (LGCES), Université 20 Août 1955, Skikda, Algeria
[e] Physical and Materials Chemistry Division, CSIR-National Chemical Laboratory, Dr. Homi Bhabha Road, Pune, 411008, India
[f] Academy of Scientific and Innovative Research, Anusandhan Bhawan, 2 RafiMarg, New Delhi 110 001, India

ARTICLE INFO

Article history:
Received 14 December 2017
Received in revised form
5 February 2018
Accepted 6 February 2018
Available online 8 February 2018

Keywords:
Protein aggregation
Calcitonin
Porous reduced graphene oxide
Electrochemistry
Disposable electrodes

ABSTRACT

In part 1 (A. Vasilescu et al., Porous reduced graphene oxide modified electrodes for the analysis of protein aggregation. Part 1: Lysozyme aggregation at pH 2 and 7.4 Electrochem. Acta, 254 (2017) 375–383) we proposed porous reduced graphene oxide coated glassy carbon electrode (GC/prGO) in combination with differential pulse voltammetry as a new analytical tool for aggregation studies of proteins. Lysozyme was used as a model to follow its aggregation by electrochemical means at pH 2 and pH 7.4, leading to the formation of amyloid and amorphous aggregates, respectively. Part 2 of this work widens the scope of this approach by investigating a biopharmaceutical product, as the aggregation of peptide based drugs affects their therapeutic activity and can induce allergic reactions in patients. The salmon polypeptide calcitonin (sCT) was chosen as an example of a bioactive peptide with limited pharmaceutical potential due to a tendency to form cytotoxic aggregates and amyloid fibrils. For practical applications, screen printed electrodes (SPE) and flexible electrodes (FE) modified with polydiallyldimethylammonium (PDDA) and prGO by using the layer-by-layer deposition technique have been developed for the detection of sCT. The results indicate that these electrodes can differentiate between formation of amyloid aggregates of calcitonin (2 mg mL^{-1}) in citrate buffer to no aggregation in acetate buffer. It was further demonstrated that these electrodes are able to analyze a pharmaceutical drug product of low potency, Miacalcic (8.3 μg mL^{-1}), where no aggregation was observed.

1. Introduction

Peptide and protein based drugs have gained considerable attention as potential therapeutics in the treatment of severe diseases such as cancer, diabetes, osteoporosis, etc. due to their high potency and specificity [1,2]. One of the major concerns in their development and use is their low stability [3]. The native functional structure of folded proteins and peptides is susceptible to physical and chemical instability, which can lead to the destruction or formation of bonds within the therapeutic molecules, altering their primary structures and affecting their higher-level architectures. To ensure enhanced stability of biopharmaceuticals, pharmaceutical excipients such as salt and buffering agents, sugars, preservatives and larger compounds including polymers are used in protein formulations [4]; however some preservatives can trigger themselves the aggregation of proteins [5]. Consequently, the stability of protein- and peptide-based drugs during manufacturing and

* Corresponding author.
** Corresponding author.
E-mail addresses: avasilescu@biodyn.ro (A. Vasilescu), sabine.szunerits@univ-lille1.fr (S. Szunerits).

https://doi.org/10.1016/j.electacta.2018.02.038
0013-4686/

storage has to be monitored to ensure their safe use. While this assessment is typically done by a combination of analytical and imaging methods, including separation based procedures (chromatography, gel electrophoresis), light scattering based methods, analytical ultracentrifugation, field-flow fractionation etc, electrochemical assays were shown to be simple complementary tools assisting with determining the native, unfolded or aggregated state of peptide/protein and its interactions with other compounds [6–14]. The direct electrochemistry of proteins/peptides relies on the electroactivity of cysteine, tyrosine, tryptophan, histidine and methionine residues in the protein and on the link between the efficiency of their oxidation and the surface exposure of these residues, according to protein conformation [15,16]. Not surprisingly, the major focus of electrochemical assays to evaluate the aggregation status of peptides/proteins was on peptides and proteins involved in neurodegenerative diseases, e.g. amyloid beta or α-synuclein [8,17–20]. In Part 1, we have introduced porous reduced graphene oxide (prGO) modified electrodes for the investigation of a model protein, lysozyme [21].

In this work, to validate that porous reduced graphene oxide (prGO) modified electrodes are suitable for the analysis of pharmaceutical formulations, the electrochemical aggregation assay was tested on a salmon calcitonin (sCT) containing pharmaceutical. Calcitonin, a polypeptide hormone which regulates the calcium-phosphorus metabolism in our body, was chosen because it represents an excellent example of a bioactive peptide with limited pharmaceutical potential due to a tendency to aggregate [22–24], leading to the formation of cytotoxic aggregates and amyloid fibrils, which can elicit important immunogenic response in patients [22]. Synthetic or recombinant human calcitonin (hCT) as well as salmon calcitonin (sCT) formulations have been used to cure metabolic bone disorders such as osteoporosis, Paget's disease, hypercalcemia of malignancy and musculoskeletal pain [25,26]. Salmon calcitonin, an approximately 50% amino acid homology to hCT [27], has been preferentially included in various pharmaceutical preparations, such as nasal sprays or parenterals, for the treatment of osteoporosis due to its longer half-life time and 40 times higher potency over hCT. While the recent association between the use of sCT and the development of cancer has prompted the suspension of calcitonin nasal sprays from the European market and limited the duration of use of other calcitonin products [28], it is currently still the active pharmaceutical ingredient in injectable calcitonin solutions for the treatment of hypercalcemia and Paget's disease.

We demonstrate in this article that next to prGO modified glassy carbon electrodes, screen printed electrodes as well as flexible integrated electrical interfaces can be modified with prGO by a layer-by-layer approach using positively charged polydiallyldimethylammonium (PDDA) and negatively charged prGO. These electrodes exhibited improved sensitivity towards sCT and could be successfully used to discriminate between sCT amyloid-type aggregation in citrate buffer and no amyloid formation in acetate buffer, respectively. The approach is further exemplified on a sCT pharmaceutical product of low potency, Miacalcic injection, containing 50 IU mL^{-1} (8.3 μg mL^{-1}) sCT in acetate buffer.

2. Experimental

2.1. Materials

Potassium hexacyanoferrate (II) ($[K_4Fe(CN)_6]$), thioflavin T (ThT), polydiallyldimethylammonium (PDDA), hydrazine hydrate and phosphate buffer tablets (PBS, 0.1 M) were purchased from Sigma-Aldrich and used as received. Graphene oxide (GO) powder was purchased from Graphenea, Spain. Thioflavin T stock solutions (500 μM) were prepared daily in PBS (0.1 M, pH 7.4) and stored at room temperature in the dark to avoid any possible photodegradation. Salmon calcitonin (sCT) was purchased from Merck, Germany. Miacalcic 50 UI mL^{-1} solution for injection and infusion produced by Novartis (UK) was obtained from a local pharmacy.

Screen-printed electrodes (SPE) including a carbon working electrode with a dimeter of 4 mm, a carbon auxiliary electrode and a Ag reference electrode were provided by Dropsens, Spain.

The preparation of porous reduced graphene oxide (prGO) is reported in Part 1 [21]. It is based on the dispersion of rGO (100 mg) in H_2O_2 (100 mL; 30%) followed by ultrasonication for 30 min and refluxing for 12 h at 60 °C.

2.2. Preparation and modification of electrodes

2.2.1. Formation of flexible electrode

Circular polyimide substrates (DuPont™ Kapton® HN) of 0.125 mm in thickness and 76.2 mm in diameter were cleaned with acetone in an ultrasonic water bath for 30 min, followed by cleaning with isopropanol for 10 min and then blown dry under a nitrogen flow. To drive off any moisture that may be present on the substrates' surface, the substrates were first dried at 110 °C overnight, then coated with bis(trimethylsilyl)amine (HMDS) in a vapor prime oven (LPIII, Yield Engineering Systems). The substrates were spin coated with AZ® nLOF 2020 negative photoresist (MicroChemicals) at 2500 rpm with an acceleration of 1000 rpm/s for 20 s. Then, they were soft baked on a hotplate at 110 °C for 60 s. The photoresist was exposed with a 365 nm i-line lamp at an energy of 66 mJ/cm^2 in a SUSS MA/BA6 mask aligner. After exposure, they were heated on a hotplate at 110 °C for 60 s to help the crosslinking of the exposed resist. The development step was achieved by soaking the photoresist in AZ® 362 MIF developer for 60 s. Then, the samples were rinsed with deionized water and blown dry with nitrogen.

The polyimide substrates were coated with 5 nm Ti, followed by 70 nm Au at a rate of 1 Å/s *via* electron-beam physical vapor deposition. Finally, the photoresist was removed by soaking polyimide substrates with Nano™ Remover PG (MicroChem) in an ultrasonic water bath for 10 min. Then, the samples were carefully rinsed with isopropanol, followed by rinsing with deionized water, and blown dry with nitrogen.

2.2.2. Modification of GC with prGO

Glassy carbon electrodes (GC, A = 0.078 cm^2) polished with alumina powder were modified by drop-casting 5 μL of a suspension of prGO (1 mg mL^{-1} in water) and drying for 24 h in an oven at 60 °C. The formed GC/prGO electrodes were immersed in 0.1 M PBS (pH 7.0) and cycled 30 times between −1.5 V and +1.1 V at a scan rate of 0.1 V s^{-1} to stabilize the interface. Thereafter, to insure good reduction of the prGO, the potential was furthermore kept at −1.5 V for 3 min.

2.2.3. Modification of screen-printed electrodes (SPE) and flexible electrodes (FE)

The electrodes were modified with prGO by first depositing 5 μL of a solution of PDDA (5% in 0.1 M NaCl/water) onto the electrode surface and allowed to adsorb for 15 min at room temperature in a humidity-saturated chamber. After rinsing and drying, a 5 μL aliquot of prGO (1 mg mL^{-1}) was deposited onto the electrode surface and allowed to adsorb in the same manner. These steps were repeated three times. Before use, the PDDA/prGO interface was cycled between −1.5 V and 0.6 V in 0.1 M PBS buffer for 10 times.

2.3. Aggregation studies

2.3.1. Salmon calcitonin (sCT) aggregation

2.3.1.1. Investigation of aggregation of 2 mg mL^{-1}sCT in citrate buffer and acetate buffer. Calcitonin solutions 2 mg mL^{-1} (0.59 mM) in two different buffers were investigated in this study: one enabling aggregation and one supposed to be stable according to a large screening work by Capelle et al. [29]. A concentration of 2 mg mL^{-1} sCT, higher than sCT based biopharmaceuticals developed so far (8.3–367 μg mL^{-1}) was chosen based on the screening study by Capelle et al. [29]. To aggregate sCT, a 2 mg mL^{-1} solution of sCT in citrate buffer (10 mM, pH 6) was kept under shaking at room temperature for 14 days. As a control, 2 mg mL^{-1} sCT were dissolved in acetate buffer (0.1 M, pH 4.2) a supposedly stable formulation [29] and kept under shaking at room temperature for several days. The acetate buffer reflected the excipients in Miacalcic injectable 50 IU mL-^{1} i.e., acetic acid, sodium acetate and sodium chloride.

2.3.1.2. Investigation of low potency sCT solutions. Aggregation of low potency sCT solutions was investigated at room temperature, under shaking: (i) Miacalcic injectable solution (containing ≈8.3 μg mL^{-1} sCT), (ii) 8.3 μg mL^{-1} sCT solution in acetate buffer (0.1 M, pH 4.2) and (iii) 8.3 μg mL^{-1} sCT solution in citrate buffer (10 mM, pH 6). The conditions and concentrations of sCT were chosen to allow observing aggregation within a reasonable timeframe (up to 10 days). Mechanical stress and temperature are among the commonly used stress factors in forced degradation studies employed in the pharmaceutical industry to assess the stability of biopharmaceuticals, when developing new products. As the aggregation of a 2 mg mL^{-1} sCT in citrate buffer (10 mM, pH 6) at room temperature under shaking occurs in some hours, for better observing the changes in the stability of this particular solution and the correlations with the electrochemical signal the shaking part was omitted for this sample. For all other calcitonin samples investigated (at 2 mg mL^{-1} in acetate and at 8 μg mL^{-1} sCT in 10 mM citrate pH 6 and in 10 mM acetate pH 4.2) the stability was studied under shaking at room temperature.

2.3.2. Fluorescence based aggregation studies

A volume of 380 μL of thioflavin T (135 μM in 0.01 M phosphate buffer pH 7.4) was mixed with 20 μL of the 2 mg mL^{-1} sCT sample, vortexed shortly, and then its fluorescence was measured with a Glomax 20/20 Luminometer from Promega equipped with a fluorescence Blue Module (excitation 465–485 nm, emission at 515–575 nm). Undiluted Miacalcic solutions were mixed in equal volumes with the thioflavin T solution before measuring the fluorescence.

2.3.3. Electrochemical-based aggregation assay

For electrochemical measurements, sCT samples were diluted (20 or 2 μg mL^{-1}) with acetate or citrate buffer just before the measurements, to be in the linear range of the calibration curves. sCT standard solutions in acetate buffer were used for calibration. The electrodes were immersed into the sCT solution and kept for 30 min to adsorb the protein onto their surface, rinsed copiously with the buffer solution, and then analyzed by differential pulse voltammetry (DPV).

2.4. Instrumentation

Scanning electron microscopic images (SEM) of the films were obtained using an electron microscope ULTRA 55 (Zeiss) equipped with a thermal field emission emitter and three different detectors (ESB detector with filter grid, high efficiency In-lens SE detector, Everhart-Thornley Secondary Electron Detector).

Electrochemical measurements were performed with a potentiostat/galvanostat (Metrohm Autolab, The Netherlands). A conventional three-electrode configuration was employed using a silver wire and a platinum mesh as reference and auxiliary electrodes, respectively. Differential pulse voltammograms (DPV) were recorded within the potential range from 0.4 V to +1.0 V under modulation amplitude of 5 mV with a step potential of 80 mV, step height of 15 mV and step time of 250 ms.

Atomic Force Microscopy (AFM) was used to observe the nature of the protein aggregates formed in the forced aggregation experiments. In order to obtain the AFM images, 20 μL aliquots of the sCT solutions (undiluted 8 μg mL^{-1} solutions or dilutions at 50 μg mL^{-1} from the 2 mg mL^{-1} solutions) were spotted onto freshly cleaved mica samples. The mica samples were then dried in a desiccator under vacuum, thoroughly washed with ultrapure water and finally dried under a flow of nitrogen. A NanoWizard II AFM instrument (from JPK Instruments AG, Germany), Arrow Silicon SPM-Sensors (with typical resonance frequency of 285 kHz and force constant of 42 N/m, from Nano World AG, Switzerland), and intermittent contact mode were used to record AFM images of the aggregates adsorbed onto the mica samples. The dimensions of the scanned area were adjusted in order to obtain representative images of a reasonable number of fibrils. The obtained AFM data was leveled by mean plane subtraction and/or corrected by matching height median.

3. Results and discussion

3.1. Direct electrochemical oxidation of sCT on glassy carbon electrodes modified with prGO

Fig. 1A depicts the differential pulse voltammogram of a solution of salmon calcitonin (sCT, 20 μg mL^{-1}) in PBS (pH 7.4, 0.1 M) after adsorption for 30 min on a glassy carbon electrode modified with prGO (GC/prGO) (for optimization of adsorption time see Fig. S1**).** It displays an oxidation peak at 0.61 V assigned to the tyrosine (Tyr) residue present on sCT [21]. The peak current at 0.61 V scales proportional with the concentration of sCT between 1 and 50 μg mL^{-1} with a coefficient of 0.9998 according to j (μA cm^{-2}) = 0.038 + 0.16 [sCT] (μg mL^{-1}) and a detection limit of 1 μg mL^{-1} sCT estimated from five blank noise signals.

3.2. Direct electrochemical oxidation on screen printed and flexible electrodes modified with rGO

For practical applications, it is advantageous to use cheap and disposable electrodes. To bring our prGO based approach closer to reality, in addition to glassy carbon electrodes we investigated commercially available screen printed electrodes (SPE) with a carbon working electrode of about 0.13 cm^2 active area and a flexible electrode (FE) design, based on a spherical gold electrode (A = 0.0095 cm^2) integrated together with a silver reference electrode and gold counter electrode onto a flexible polymer support (Fig. 2A). Integration of prGO onto these interfaces was achieved by a layer-by-layer deposition approach [30] using subsequently positively charged PDDA and negatively charged prGO. Fig. 2B exhibits the surface morphology of the SPE and FE before and after modification with one and several of PDDA/prGO layers. In the case of SPE, the deposition of 4 PDDA/prGO layers results in an electrode surface completely covered with prGO, whereas in the case of the flexible interfaces, 3 layers of PDDA/prGO coat evenly the interface. The electrochemical responses of both electrical interfaces before and after PDDA/prGO modification were recorded (see SI, Fig. S1). Enhanced electron transfers with a ΔE = 86 mV and larger current

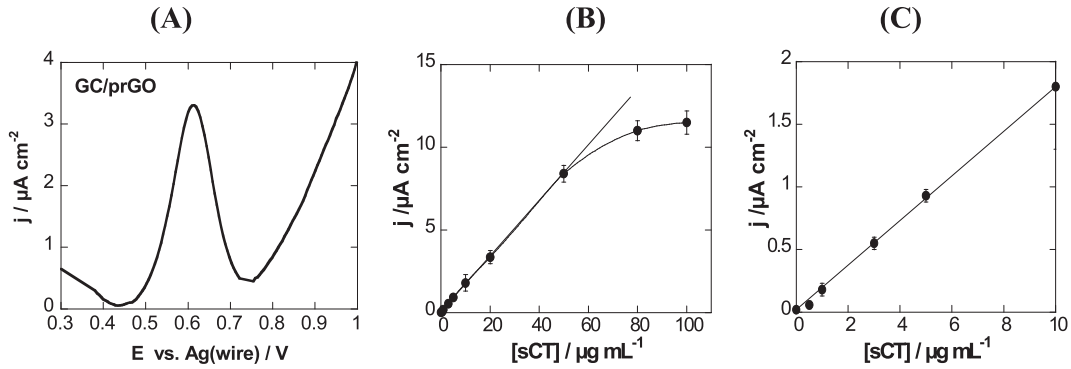

Fig. 1. (A) Differential pulse voltammogram of sCT (20 µg mL^{-1}) after 30 min adsorption onto GC/prGO in acetate buffer, scan rate = 100 mV s^{-1}; (B) Calibration curves for sCT (0–100 µg mL^{-1}) and (C) zoom to lower concentrations (0–10 µg mL^{-1}).

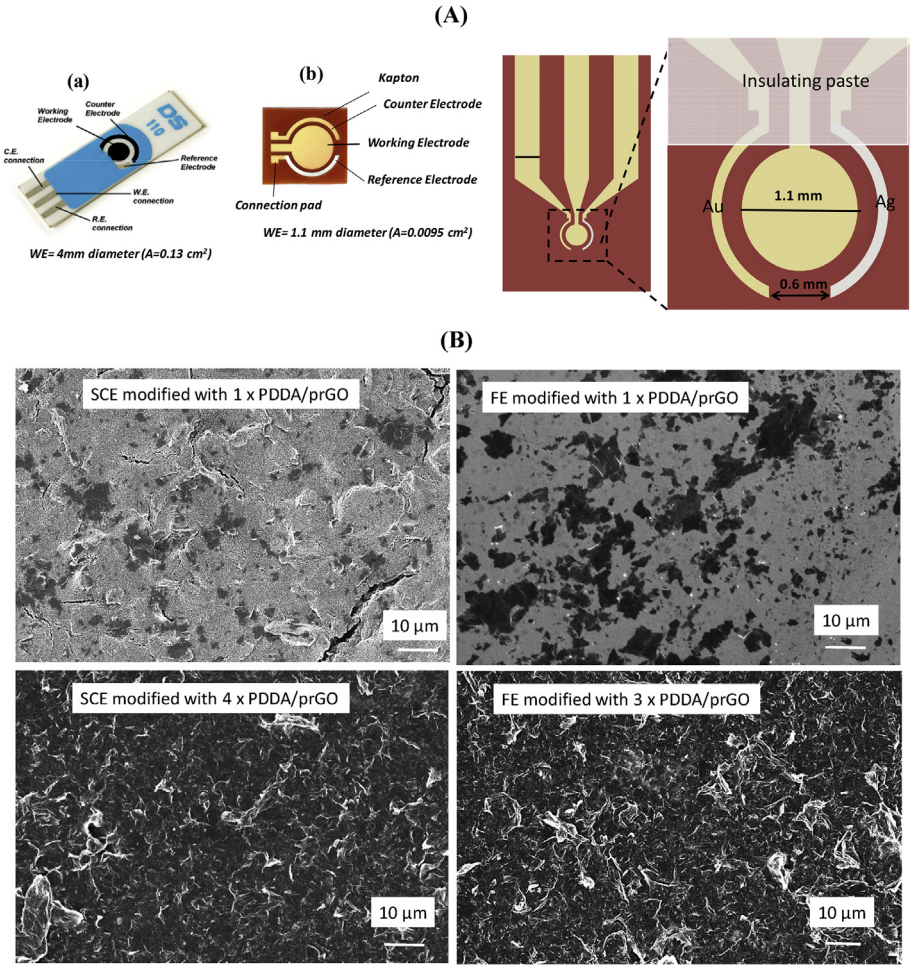

Fig. 2. (A) Images of screen printed electrodes (SPE) and flexible gold electrodes (FE); (B) SEM images of SPE and FE before and after modification with PDDA/prGO.

densities are observed on SPE-$(PDDA/prGO)_4$ when compared to unmodified SPE. Additional layers showed only a slight increase of the current density. In the case of the FE, coating with three layers of PDDA/prGO results in enhanced current densities and a good electron transfer is retained.

The influence of the number of PDDA/prGO layers on the electrochemical response towards sCT was in addition investigated. After 30 min adsorption of 5 µL of sCT and rinsing, DPVs were recorded (Fig. 3A). Increased peak currents are detected on SPE-$(PDDA/prGO)_4$ and FE-$(PDDA/prGO)_3$ when compared to unmodified SPE and FE and when coated with only one layer of PDDA/prGO. Well-defined oxidative bands are observed at 0.64 V on SPE and 0.61 V on FE, assigned to the oxidation of tyrosine residue in calcitonin. On PDDA/prGO modified interfaces the redox band is shifted cathodically to 0.61 and 0.57 V for SPE-$(PDDA/prGO)_4$ and FE-$(PDDA/prGO)_3$ respectively. In the case of SPE-$(PDDA/prGO)_4$, the peak current at 0.60 V scales linearly between 0.2 and 80 µg mL^{-1} with a coefficient of 0.9994 according to j (µA

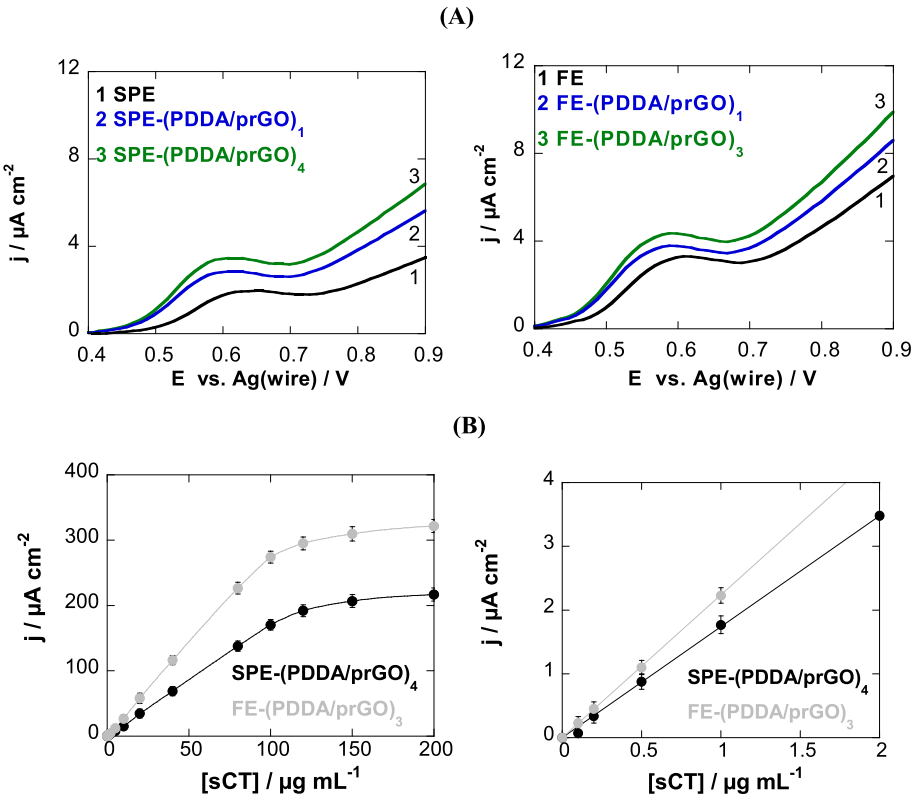

Fig. 3. (A) Differential pulse voltammograms of sCT (2 µg mL^{-1}) after 30 min adsorption onto SPE and FE interfaces and when modified with one or more layers of PDDA/prGO in acetate buffer, scan rate = 100 mV s^{-1}; (B) Calibration curves for sCT for both interfaces (0–200 µg mL^{-1}) and a zoom to lower concentrations (0–2 µg mL^{-1}).

cm^{-2}) = 0.188 + 1.714 [sCT] (µg mL^{-1}) and a detection limit of 0.1 µg mL^{-1} estimated from five blank noise signals was achieved. When compared to GC/prGO, the linear range is enlarged on these electrical interfaces with a detection limit lowered by one order of magnitude.

Somewhat improved performances were recorded with the FE-(PDDA/prGO)$_3$ interface with a linear range between 0.1 and 100 µg mL^{-1} according to j (µA cm^{-2}) = 0.128 + 2.81 [sCT] (µg mL^{-1}) with a detection limit of 0.08 µg mL^{-1} estimated from five blank noise signals. This concentration range is well adapted for the investigation of pharmaceutical samples such as the Miacalcic injectable solution from Novartis, which contains about 8.3 µg mL^{-1} of sCT.

3.3. Salmon calcitonin (sCT) aggregation studies

When proteins unfold, the number of surface-exposed electroactive amino acids available for direct electrochemical oxidation changes. This has been intensively discussed in Part 1 using lysozyme as a model compound [21]. Here we investigate if this concept is applicable to sCT aggregation knowing that this molecule comprises electrochemical active amino acids (1 tyrosine, 1 histidine and 2 cysteine residues linked through a disulfide bridge) in its structure. Aggregation of sCT (2 mg mL^{-1}) at room temperature under shaking in acetate buffer as well as in citrate buffer (without shaking) was followed electrochemically using GC/prGO, SPE-(PDDA/prGO)$_4$ and FE-(PDDA/prGO)$_3$ electrodes. As can be seen from Fig. 4A, after an increase in the current density reaching a plateau after 50 h, the electrochemical response decreases. Various studies, including tyrosine, tyrosine-containing peptides, peptide isoforms and inverse peptides, have shown that the electrochemical signal of tyrosine (or other electroactive amino acids) in peptides and proteins is influenced by neighboring amino acid residues and by the secondary structure of proteins [6,31–33], determining surface exposure and accessibility for oxidation of tyrosine, adsorption and secondary reactions. In a simplistic interpretation of the evolution of the current density in Fig. 4A, the current density is determined by major contributions from monomeric unfolding sCT contributing to the increase in current in the first 50 h and the depletion of sCT monomers with formation of high amount of fibrils for long aggregation time. Indeed, the increase in the electrochemical signal at 0.61 V in the first 50 h of aggregation is attributed to the unfolding of calcitonin, resulting in the surface exposure of different amino acids compared to the native conformation and to an easier accessibility of tyrosine for oxidation at electrode surface. The conformational changes also result in the modification of the hydrophobicity of sCT as verified by measurements with the fluorescent probe 8-anilino-1-sulphonate (see SI, Fig. S2). The results show that there are large variations in surface hydrophobicity of sCT during the first 2 days. Modified hydrophobicity is anticipated to influence the adsorption of sCT on the electrodes, thus indirectly contributing to the electrochemical signal. These modifications lead to more important adsorption or more favorable exposure of tyrosine residues, resulting in the higher oxidation current densities in the first 50 h of aggregation (Fig. 4A). After 72 h of aggregation, the formation of oligomers and aggregates lead to tyrosine being hidden inside the polypeptide structure, shielded by non-electroactive amino acids, resulting in its inaccessibility for oxidation at electrode surface-hence a marked decrease of the electrochemical signal with time. The loss of electrochemical signal was complete after 250 h of aggregation. The same trend was observed using SPE-(PDDA/prGO)$_4$ and FE-(PDDA/prGO)$_3$ electrodes (Fig. 4B). In the case of FE-(PDDA/prGO)$_3$, the loss in electrochemical signal after 50 h is more pronounced than in the

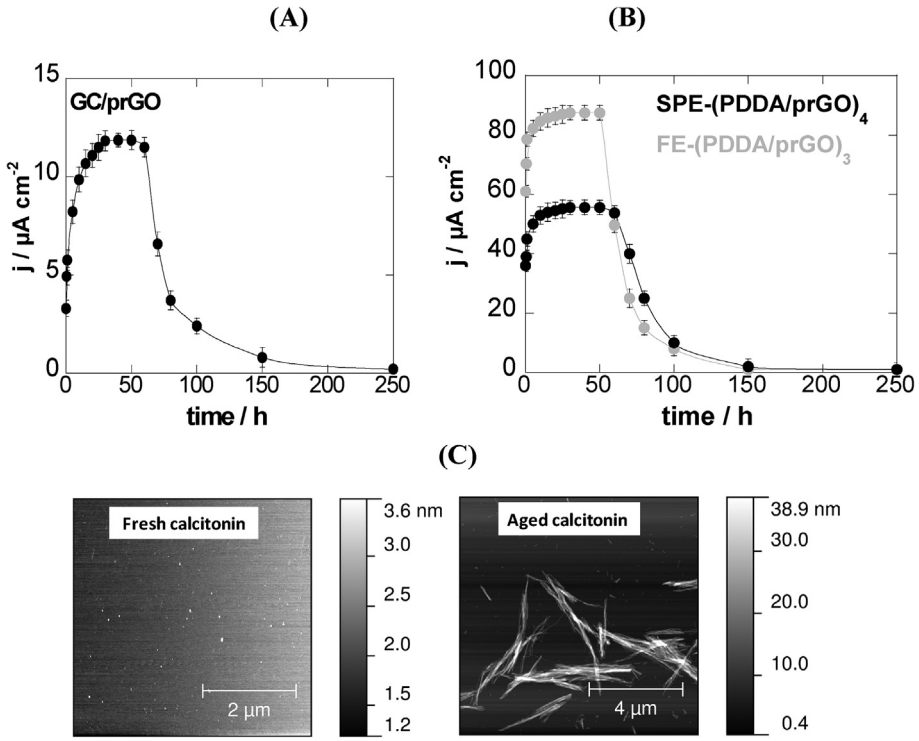

Fig. 4. Change in peak current densities of a sCT solution (2 mg mL^{-1}) in citrate buffer (diluted to 20 µg mL^{-1} to be in linear range of calibration curve) at different time intervals on a (A) GC/prGO electrode, (B) SCE-(PDDA/prGO)$_4$ and FE-(PDDA/prGO)$_3$ (**C**) AFM images of fresh calcitonin and after aging in citrate buffer for 72 h.

other cases most likely due to the higher sensitivity of the interface.

The formation of amyloid aggregates in citrate buffer occurring after 72 h in sCT solution (2 mg mL^{-1} in citrate buffer) was confirmed by AFM measurements (Fig. 4C). The diameter of single calcitonin fibrils is rather large with a mean diameter 5.8 ± 1.4 nm along with a wide distribution of the fibril diameters. The calcitonin fibrils also tend to laterally associate to each other and form ribbon-like structures.

Several authors have attempted to correlate the electrochemical signals with the size of aggregates measured by AFM [9] or Dynamic Light Scaterring (DLS) [12,17]. For example Suprun et al. have used (DLS) and fluorescence of thioflavin T in conjunction with square wave voltammetry to study the aggregation of Aβ42 [17]. The authors found that the magnitude of the current is manly dictated by the monomer amount and once aggregation has progressed so much that aggregates larger than 35 nm are formed, the current due to Aβ42 oxidation decreases linearly with the magnitude of aggregates. It is important to point out however that the electrochemical signal reflects the global contributions from the aggregated solution which contains, at any given time-point, different amounts of monomer, degradation products, oligomers and aggregates. In our case, identifying the specific contributions to the electrochemical signal exclusively due to sCT aggregates requires both highly stable aggregates and a combination of several analytical methods.

To support some of our claims, we have used thioflavin T fluorescence measurements as second analytical method and compared the aggregation in citrate buffer with a stability study of a 2 mg mL^{-1} sCT solution in acetate buffer. Thioflavin T is a benzothiazole dye that binds to β-sheets which are characteristic and abundant in amyloid-type aggregates. For 2 mg mL^{-1} sCT solutions in citrate buffer (1 mM, pH 6) kept at room temperature with no stirring, the fluorescence based assay gave a strong ThT emission reaching a plateau after about 4 days with a lag time of 1 day. The high fluorescence signal after 3–4 days is in line with the amyloid fibers observed by AFM and supports the link between a high amount of amyloid aggregates and the loss of electrochemical signal as observed by DPV.

In contrast to results in citrate buffer, the fluorescence signal of thioflavin T mixed with 2 mg mL^{-1} sCT solutions in acetate buffer increases only by approximately 10% from the initial value (Fig. 5A). The solution remains clear after 5 days and the change in electrochemical signal recorded by DPV is small (Fig. 5B), indicating that acetate-based sCT formulations are long-time stable against aggregation, in accordance to literature-reported data [29].

In conclusion, the electrodes reported here can detect changes in peptide conformation and in solution composition that precede and accompany the formation of aggregates. The results obtained with 2 mg mL^{-1} sCT solutions in citrate and acetate are indicative of the potential of SPE-(PDDA/prGO)$_4$ and FE-(PDDA/prGO)$_3$ electrodes and the manner of their application for stability studies and formulation development in the biopharmaceutical industry. We believe the electrodes to be useful, complementary tools in combination with optical methods [34] for the screening of pharmaceutical formulations.

3.4. Aggregation studies of a pharmaceutical sCT containing product

Protein aggregation strongly depends on the experimental conditions such as protein concentration type of buffer solution, pH, temperature shaking and many others. To achieve protein stabilization through retardation of chemical degradation processes and prevention of aggregation various excipients are included in pharmaceutical formulations. Some excipients might interfere with the electrochemical approach described here. For example, phenol, and m-cresol are two preservatives used to increase the antimicrobial stability of drugs based on therapeutic

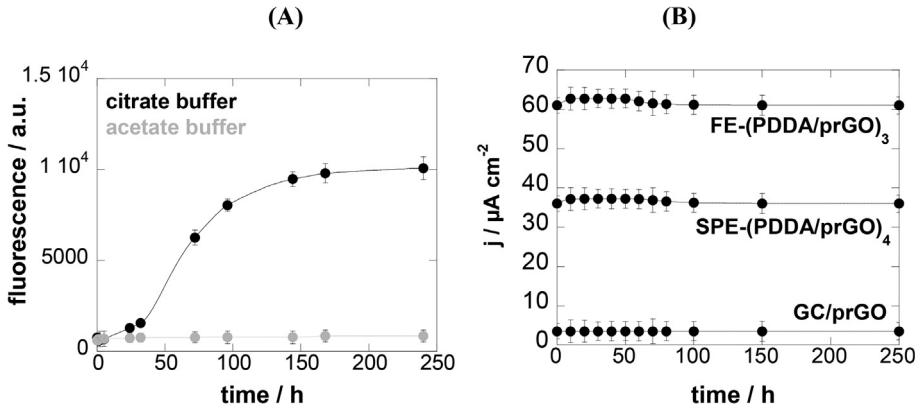

Fig. 5. (A) ThT fluorescence intensity upon aging a solution of sCT (2 mg mL^{-1}) in citrate buffer (black) or acetate buffer (gray) at room temperature; (B) Change of peak current density with time recorded on GC/prGO, SPE-(PDDA/prGO)$_4$ and FE-(PDDA/prGO)$_3$ electrodes upon aging of a sCT solution (2 mg mL^{-1}) in acetate buffer (diluted to 20 µg mL^{-1} to be in linear range of calibration curve).

peptides and are used as preservatives in various calcitonin parenterals and nasal sprays. Due to their chemical structures, these compounds have similar redox properties as tyrosine and might potentially interfere with electrochemical tyrosine oxidation in sCT. As illustrated in Fig. S3, phenol and metacresol interfere with the direct oxidation of sCT as they are oxidized at similar potentials as the tyrosine residue in calcitonin. However, some biopharmaceuticals do not include preservatives, as is the case of Miacalcic vials for injection with a potency of 50 IU mL^{-1} calcitonin studied here [35], in contrast to higher potency Miacalcin injectable drugs which do contain phenol as preservative [36]. Moreover, there are significant efforts nowadays towards developing preservative-free formulations as the compounds chosen to enhance the stability of proteins were found in some case to induce themselves the protein aggregation [5]. Taken together, these facts justify our choice to study Miacalcic 50 IU mL^{-1} aggregation.

Before investigating the stability of Miacalcic 50 IU mL^{-1}, we performed aggregation studies with sCT solutions prepared in the laboratory at the same concentration (8.35 µg mL^{-1}) and in acetate buffer (pH 4.2) mimicking the formulation of Miacalcic. Under these conditions, no significant decrease, indicative of aggregation was observed with either the SPE-(PDDA/prGO)$_4$ or FE-(PDDA/prGO)$_3$ electrode (Fig. 6A). No visible aggregates were observed in the sample solution at the end of the study.

The same behavior is recorded for the Miacalcic 50 IU mL^{-1} formulations: although the intensity of the oxidation current displayed some variations throughout the 250 h study, there is no significant decrease in the current density over the course of 5 days at room temperature, under shaking (Fig. 6B), a sign of a lack of aggregation. The observed variations in current densities deserve further investigation in a future work with parallel analysis (e.g by chromatography, circular dichroism etc) to correlate with conformational modifications or product degradation. Obviously, the sensitivity of SPE-(PDDA/prGO)$_4$ and FE-(PDDA/prGO)$_3$ recommend them as complementary analytical tools for such aggregations studies.

Fluorescence was used as second analytical method to confirm the absence of amyloid aggregates in the pharmaceutical drug product (Fig. 6C) where indeed no change in fluorescence was observed. The apparent stability of the Miacalcic solution and of 8.35 µg mL^{-1} sCT in acetate is not surprising, considering the similar results obtained with 2 mg mL^{-1} sCT solution (240 times more concentrated, see Fig. 5B) and that the speed of the aggregation process is influenced by the concentration of the monomer, proceeding slower for lower concentrations. With respect to the last, we have verified that while for sCT prepared in citrate buffer (10 mM, pH 6) where aggregation is promoted, amyloid formation occurs fast in a 2 mg mL^{-1} solution, in the case of a 8 µg mL^{-1} sample it starts being observed only after 14 days of shaking at room temperature, as emphasized by electrochemical, fluorescence and AFM procedures (see SI, Figure S4). Bundles of short fibrils are visible by AFM analysis, similarly to images recorded for 2 mg mL^{-1} calcitonin solutions aggregated 3 days (Fig. 4C). For a 8 µg mL^{-1} calcitonin in 10 mM citrate pH 6 aggregated 14 days the increase in fluorescence of thioflavin T is significant after 14 days (532 ± 37 FLU at day 14 compared to 431 ± 3 FLU initially) and correlates with the fibrils observed by AFM.

This work with prGO-modified disposable electrodes complements the current knowledge on the application of electrochemical methods for peptide and protein detection and for the study of interactions and aggregation, particularly with concern of the development of novel, more performant and cost-effective interfaces. While very sensitive assays for calcitonin were reported based on molecular imprinted polymers or antibodies, reaching detection limits of 0.7 pg mL^{-1} [37], and 3.09 pg mL^{-1}) [38], respectively, the direct electrochemical detection of calcitonin is less studied [39,40]. Oesteryoung reported the square wave adsorptive stripping voltammetry of salmon calcitonin at hanging mercury drop electrodes with a detection limit of 343 pg mL^{-1} [39]. Glassy carbon electrodes were largely used for the study of protein aggregation and their electrochemistry [32,41], including in recent works reporting on the antibody drugs Rituximab and Bevacizumab [42,43]. Boron-doped diamond electrodes [44] were used in protein electrochemistry studies and a few works were based on screen-printed carbon electrodes [45]. No works were yet reported with flexible electrodes and prGO-modified interfaces. With regards to calcitonin aggregation, a great deal of knowledge on human and salmon calcitonin and their pharmaceutical formulations was acquired by optical assays and imaging methods [29] and the subject continues to be of interest [46], however none of these reports included an electrochemically-based assessment.

4. Conclusion

This study reports on the development of different electrochemical interfaces for the sensitive detection of salmon calcitonin. Next to glassy carbon electrodes modified with prGO by drop coating, screen printed electrodes as well as flexible electrodes were modified with prGO using a layer-by-layer approach alternating PDDA and prGO. Compared to GC/prGO, these interfaces

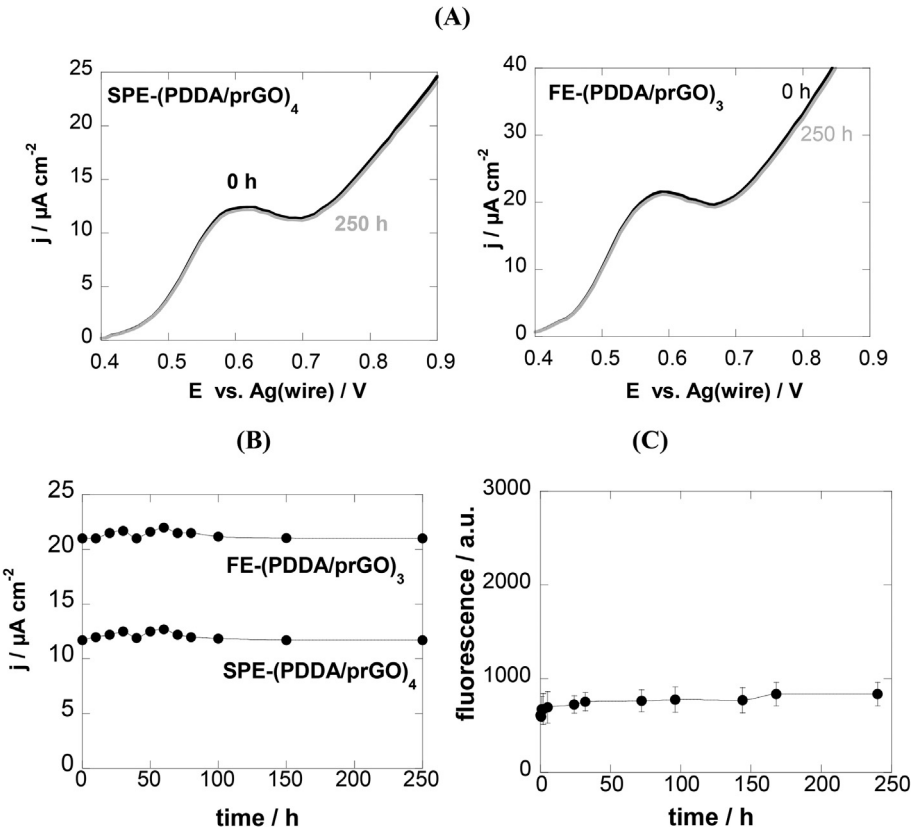

Fig. 6. (A) Change in differential pulse voltammograms upon aging of sCT solution (8.35 µg mL^{-1}) in acetate buffer (0.1 M, pH 4.2) under shaking at room temperature, recorded with SPE-(PDDA/prGO)$_4$ and FE-(PDDA/prGO)$_3$ electrodes; (B) Change of peak current density with time recorded upon aging Miacalcic 50 IU mL^{-1} (8.35 µg mL^{-1}) calcitonin solution under shaking; (C) ThT fluorescence intensity upon aging Miacalcic 50 IU mL^{-1} calcitonin solution under shaking.

showed an improved detection limit towards sCT oxidation as well as an wider linear range up to 100 µg mL^{-1}. These electrodes proved to be adaptable to investigate aggregation of sCT under different conditions as well as to monitor the stability of a low potency sCT pharmaceutical product. It was found that sCT is stable in acetate-based solutions, while aggregation is spontaneously occurring in citrate buffer at pH 6. The Miacalcic pharmaceutical product showed no aggregation as the low concentration of sCT together with being solubilized in acetate buffer results in a stable pharmaceutical solution. Acknowledging the limitations related to possible interferences due to electroactive excipients, there is a good deal of applicability in our proposed approach which could be extended to other therapeutic peptides or formulations. Thanks to their good sensitivity, the proposed electrodes could function for example as detectors in conjunction with a separation-based method, e. g chromatography. More importantly, since they allow observing changes in the stability of biopharmaceuticals such as calcitonin, at concentrations ranges typically used in the pharmaceutical industry, the prGO-based electrodes can be used during the drug development process. For example, they can be useful in forced degradation studies as part of screening various formulations and excipients and for validating the storage and processing of the active pharmaceutical peptide/protein.

This electrochemical approach is thus proposed as a general and easy manner, complementary to available analytical techniques to get information about the aggregation behavior of protein therapeutics in short time, using rather cheap instrumentation and electrical interfaces.

Acknowledgements

Financial support from the Centre National de la Recherche Scientifique (CNRS), the University of Lille, the Hauts-de-France region, the CPER “Photonics for Society”, and the joint support of Agence Nationale de la Recherche and of Executive Agency for Higher Education, Research, Development and Innovation Funding (UEFISCDI) through FLAG-ERA JTC 2015-Graphtivity project are acknowledged.

Appendix A. Supplementary data

Supplementary data related to this article can be found at https://doi.org/10.1016/j.electacta.2018.02.038.

References

[1] K. Fosgerau, T. Hoffmann, Peptide therapeutics: current status and future directions, Drug Discov. Today 20 (2015) 122–128.
[2] B.J. Bruno, G.D. Miller, C.S. Lim, Basics and recent advances in peptide and protein drug delivery, Ther. Deliv. 4 (2013) 1443–1467.
[3] S. Frokjaer, D.E. Otzen, Protein drug stability: a formulation challenge, Nat. Rev. Drug Discov. 4 (2005) 298–306.
[4] T.J. Kamerzell, R. Esfandiary, S.B. Joshi, C.R. Middaugh, D.B. Volkin, Protein-excipinet interactions: mechanisms and biophysical characterization applied to protein formulation developments, Adv. Drug Deliv. Rev. 63 (2011) 1118–1159.
[5] R.L. Bis, K.M.G. Mallela, Antimicrobial preservatives induce aggregation of interferon alpha-2a: the order in which preservatives induce protein aggregation is independent of the protein, Int. J. Pharm. 472 (0) (2014) 356–361.
[6] T.A. Enache, A.M. Chiorcea-Paquim, A.M. Oliveira-Brett, Amyloid–β peptides time-dependent structural modifications: AFM and voltammetric characterization, Anal. Chim. Acta 926 (2016) 36–47.
[7] T.A. Enache, A.M. Oliveira-Brett, Alzheimer's disease amyloid beta peptides

in vitro electrochemical oxidation, Bioelectrochemistry 114 (2017) 13–23.
[8] P. Lopes, H. Dyrnesli, N. Lorenzen, D. Otzen, E.E. Ferapontova, Electrochemical analysis of the fibrillation of Parkinson's disease alpha-synuclein, Analyst 139 (4) (2014) 749–756.
[9] P. Lopes, M. Xu, M. Zhang, T. Zhou, Y. Yang, C. Wang, E.E. Ferapontova, Direct electrochemical and AFM detection of amyloid-[small beta] peptide aggregation on basal plane HOPG, Nanoscale 6 (14) (2014) 7853–7857.
[10] M. Masařík, A. Stobiecka, R. Kizek, F. Jelen, Z. Pechan, W. Hoyer, T.M. Jovin, V. Subramaniam, E. Paleček, Sensitive electrochemical detection of native and aggregated α-synuclein protein involved in Parkinson's disease, Electroanalysis 16 (13–14) (2004) 1172–1181.
[11] V. Ostatná, H. Černocká, K. Kurzątkowska, E. Paleček, Native and denatured forms of proteins can be discriminated at edge plane carbon electrodes, Anal. Chim. Acta 735 (2012) 31–36.
[12] E.V. Suprun, S.A. Khmeleva, Y.Y. Kiseleva, S.P. Radko, A.I. Archakov, V.V. Shumyantseva, Quantitative aspects of electrochemical detection of amyloid-β aggregation, Electroanalysis 28 (9) (2016) 1977–1983.
[13] A.J. Velosco, V.W.S. Hung, G. Sindhu, S. Costantinof, K. Kerman, Electrochemical Oxidation of benzothiazole dyes for monitoring amyloid formation related to the Alzheimer's diesease, Anal. Chem. 81 (2009) 9410–9415.
[14] N. Zhou, Z. Chen, D. Zhang, G. Li, Electrochemical assay of human islet amyloid polypeptide and its aggregation, Sensors (Basel, Switzerland) 8 (9) (2008) 5987–5995.
[15] V. Brabec, V. Mornstein, Electrochemical behaviour of proteins at graphite electrodes. II. Electrooxidation of amino acids, Biophys. Chem. 12 (2) (1980) 159–165.
[16] B. Malfoy, J.A. Reynaud, Electrochemical investigations of amino acids at solid electrodes: Part II. Amino acids containing no sulfur atoms: tryptophan, tyrosine, histidine and derivatives, J. Electroanal. Chem. 114 (2) (1980) 213–223.
[17] E.V. Suprun, S.A. Khmeleva, S.P. Radko, A.I. Archakov, V.V. Shumyantseva, Electrochemical analysis of amyloid-β domain 1-16 isoforms and their complexes with Zn(II) ions, Electrochim. Acta 187 (2016) 677–683.
[18] E.V. Suprun, N.V. Zaryanov, S. Radko, A. Kulikova, S. Kozin, A.A. Makarov, A.I. Archakov, V. Shumyantseva, Tyrosine based electrochemical analysis of amyloid-β fragment (1-16) binding to metal(II) ions, Electrochim. Acta 179 (2015) 93–99.
[19] A. Veloso, K. Kerman, Advances in electrochemical detection for study of neurodegenerative disorders, Anal. Bioanal. Chem. 405 (17) (2013) 5725–5741.
[20] E. Palecek, V. Ostatna, M. Masarik, C.W. Bertoncini, T.M. Jovin, Changes in interfacial properties of [small alpha]-synuclein preceding its aggregation, Analyst 133 (1) (2008) 76–84.
[21] A. Vasilescu, S. Boulahneche, F. Chekin, S. Gáspár, M.S. Medjram, A.A. Diagne, S.K. Singh, S. Kurungot, R. Boukherroub, S. Szunerits, Porous reduced graphene oxide modified electrodes for the analysis of protein aggregation. Part 1: lysozyme aggregation at pH 2 and 7.4, Electrochem. Acta 254 (2017) 375–383.
[22] M. Diociaiuti, M.C. Gaudiano, F. Malchiodi-Albedi, The slowly aggregating salmon Calcitonin: a useful tool for the study of the amyloid oligomers structure and activity, Int. J. Mol. Sci. 12 (12) (2011) 9277–9295.
[23] S.B. Fowler, S. Poon, R. Muff, F. Chiti, C.M. Dobson, J. Zurdo, Rational design of aggregation-resistant bioactive peptides: reengineering human calcitonin, Proc. Natl. Acad. Sci. U. S. A 102 (2005) 10105–10110.
[24] C. Guo, L. Ma, Y. Zhao, A. Peng, B. Cheng, Q. Zhou, L. Zheng, K. Huan, Inhibitory effects of magnolol and honokiol on human calcitonin aggregation, Sci. Rep. 5 (2015) 3556.
[25] S.B. Fowler, S. Poon, R. Muff, F. Chiti, C.M. Dobson, J. Zurdo, Rational design of aggregation-resistant bioactive peptides: reenginerring human calcitonin, Proc. Natl. Acad. Sci. U. S. A 102 (2005) 10105–10110.
[26] M. Azria, D.H. Copp, J.M. Zanelli, 25 years of salmon calcitonin: from synthesis to therapeutic use, Calcif. Tissue Int. 57 (1995) 405–408.
[27] H.D. Niall, H.T. Keutmann, D.H. Copp, J.T. Potts, Amino acid sequence of salmon ultimobranchial calcitonin, Proc. Natl. Acad. Sci. U. S. A 64 (1969) 771–778.
[28] G. Wells, J. Chernoff, J.P. Gilligan, D.S. Krause, Does salmon calcitonin cause cancer? A review and meta-analysis, Osteoporos. Int. 27 (2016) 13–19.
[29] M.A.H. Capelle, R. Gurny, T. Arvinte, A high throughput protein formulation platform: case study of salmon calcitonin, Pharma Res. 26 (1) (2008) 118–128.
[30] A. Vasilescu, S. Gaspar, M. Gheorghiu, S. David, V. Dinca, S. Peteu, Q. Waqng, M. Li, R. Boukherroub, S. Szunerits, Surface Plasmon Resonance based sensing of lysozyme in serum on Micrococcus lysodeikticus-modified graphene oxide surfaces, Biosens. Bioelectron. 49 (2017) 525–531.
[31] K. Kerman, M.D. Vestergaard, M. Chikae, S. Yamamura, E. Tamiya, Label-free electrochemical detection of the phosphorylated and non-phosphorylated forms of peptides based on tyrosine oxidation, Electrochem. Commun. 9 (2007) 976–980.
[32] E. Paleček, J. Tkáč, M. Bartošík, T. Bertók, V. Ostatná, J. Paleček, Electrochemistry of nonconjugated proteins and glycoproteins. Toward sensors for biomedicine and glycomics, Chem. Rev. 115 (5) (2015) 2045–2108.
[33] J. Roeser, H.P. Permentier, A.P. Bruins, R. Bischoff, Electrochemical oxidation and cleavage of tyrosine- and tryptophan-containing tripeptides, Anal. Chem. 82 (18) (2010) 7556–7565.
[34] M.A. Capelle, R. Gurny, T. Arvinte, A high throughput protein formulation platform: case study of salmon calcitonin, Pharm. Res. 26 (1) (2009) 118–128.
[35] R. National Drug Agency, Authorisarion to Place on the Market No. 5400/2005/01, Annex, Leaflet: User Information, 2015. Miacalcic 50 UI/ml injectable solution (document in Romanian), https://www.anm.ro/_/_PRO/pro_5400_07.06.05.pdf (Accessed 12 December 2017).
[36] Novartis, Miacalcin (Calcitonin, Salmon) Injection, Synthetic, 2011. https://www.accessdata.fda.gov/drugsatfda_docs/label/2012/017808s034lbl.pdf (Accessed 14 December 2017).
[37] N.A. Alarfaj, M.F. El-Tohamy, A label-free electrochemical immunosensor based on gold nanoparticles and graphene oxide for the detection of tumor marker calcitonin, New J. Chem. 41 (19) (2017) 11029–11035.
[38] S. Patra, E. Roy, R. Madhuri, P.K. Sharma, Imprinted ZnO nanostructure-based electrochemical sensing of calcitonin: a clinical marker for medullary thyroid carcinoma, Anal. Chim. Acta 853 (2015) 271–284.
[39] J.G. Osteryoung, K.J. Wikiel, Determination of salmon calcitonin by square wave adsorptive stripping voltammetry, Anal. Chim. Acta 351 (1) (1997) 65–71.
[40] H.S. Lee, S.J. Choi, H.M. Lee, C.K. Jeong, S.B. Kim, J.T. Lee, S.D. Yoo, P.P. DeLuca, K.C. Lee, Determination of salmon calcitonin in formulations by high-performance liquid chromatography with electrochemical detection, Chromatographia 50 (11) (1999) 701–704.
[41] I.P. Fernandes, A.M. Oliveira-Brett, Calcium-induced calmodulin conformational change. Electrochemical evaluation, Bioelectrochemistry 113 (2017) 69–78.
[42] S.C.B. Oliveira, I.B. Santarino, A.M. Oliveira-Brett, Direct electrochemistry of native and denatured anticancer antibody Rituximab at a glassy carbon electrode, Electroanalysis 25 (4) (2013) 1029–1034.
[43] F.Z. Issaad, L.I.N. Tomé, N.V. Marques, C. Mouats, V.C. Diculescu, A.M. Oliveira-Brett, Bevacizumab anticancer monoclonal antibody: native and denatured redox behaviour, Electrochim. Acta 206 (2016) 246–253.
[44] M. Chiku, K. Horisawa, N. Doi, H. Yanagawa, Y. Einaga, Electrochemical detection of tyrosine derivatives and protein tyrosine kinase activity using boron-doped diamond electrodes, Biosens. Bioelectron. 26 (2010) 235–240.
[45] E.V. Suprun, S.P. Radko, S.A. Khmeleva, V.A. Mitkevich, A.I. Archakov, A.A. Makarov, V.V. Shumyantseva, Electrochemical oxidation of amyloid-beta peptide isoforms on carbon screen printed electrodes, Electrochem. Commun. 75 (2017) 33–37.
[46] F. Rigoldi, P. Metrangolo, A. Redaelli, A. Gautieri, Nanostructure and stability of calcitonin amyloids, J. Biol. Chem. 292 (18) (2017) 7348–7357.

Supplementary Material

Porous reduced graphene oxide modified electrodes for the analysis of protein aggregation. Part 2: Application to the analysis of calcitonin containing pharmaceutical formulation

Alina Vasilescu,[a*] Ran Ye,[b] Samia Boulahneche,[c,d] Sabrina Lamraoui,[c,d] Roxana Jijie,[c] Mohamed Salah Medjram,[d] Szilveszter Gáspár,[a] Santosh K. Singh,[e,f] Sreekumar Kurungot, [e,f] Sorin Melinte,[b] Rabah Boukherroub,[c] Sabine Szunerits[c*]

[a] *International Center of Biodynamics, 1B Intrarea Portocalelor, Bucharest 060101, Romania*

[b] *Institute of Information and Communication Technologies, Electronics and Applied Mathematics, Université catholique de Louvain, 1348 Louvain-la-Neuve, Belgium*

[c] *Uni. Lille, CNRS, Centrale Lille, ISEN, Uni. Valenciennes, UMR 8520-IEMN, F-59000 Lille, France*

[d] *Laboratoire de Génie Chimique et Environnement de Skikda (LGCES), Université 20 Août 1955-Skikda, Algérie.*

[e] *Physical and Materials Chemistry Division, CSIR-National Chemical Laboratory, Dr. Homi Bhabha Road, Pune 411008, India*

[f] *Academy of Scientific and Innovative Research, Anusandhan Bhawan, 2 RafiMarg, New Delhi 110 001, India*

[*]Corresponding authors: avasilescu@biodyn.ro and sabine.szunerits@univ-lille1.fr

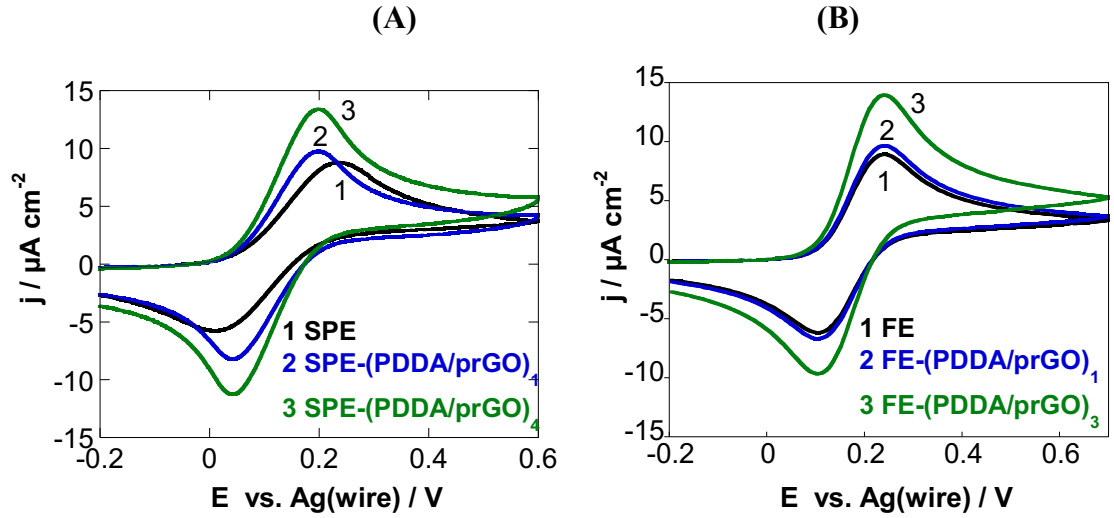

Figure S1: Cyclic voltammograms of (A) SPE and (B) FE modified with one or several layers of PDDA/prGO in $Fe(CN)_6^{4-}$ (10 mM/ PBS (0.1 M, pH 7.4), scan rate: 100 mV s^{-1}.

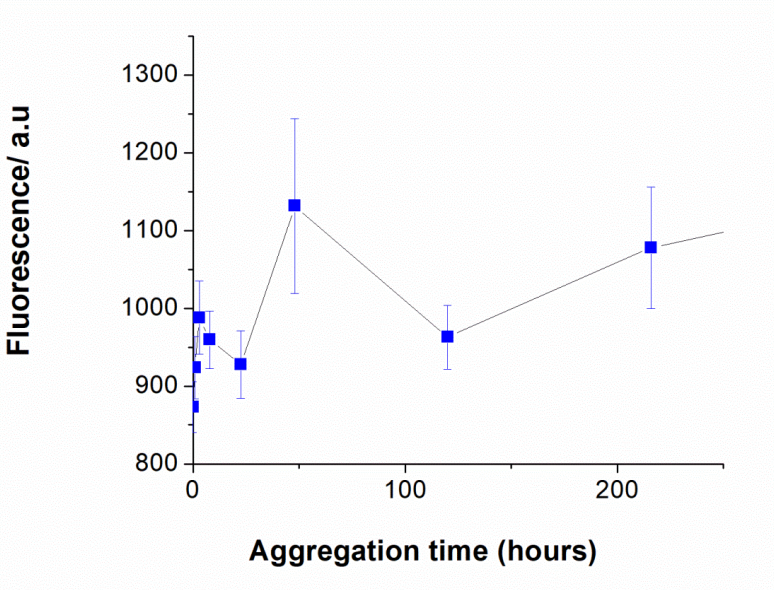

Figure S2. Fluorescence of the hydrophobicity probe 8-anilino-1-sulphonate mixed with a 2 mg mL^{-1} sCT (10 mM citrate buffer, pH 6) that was kept at room temperature for increasing periods of time;

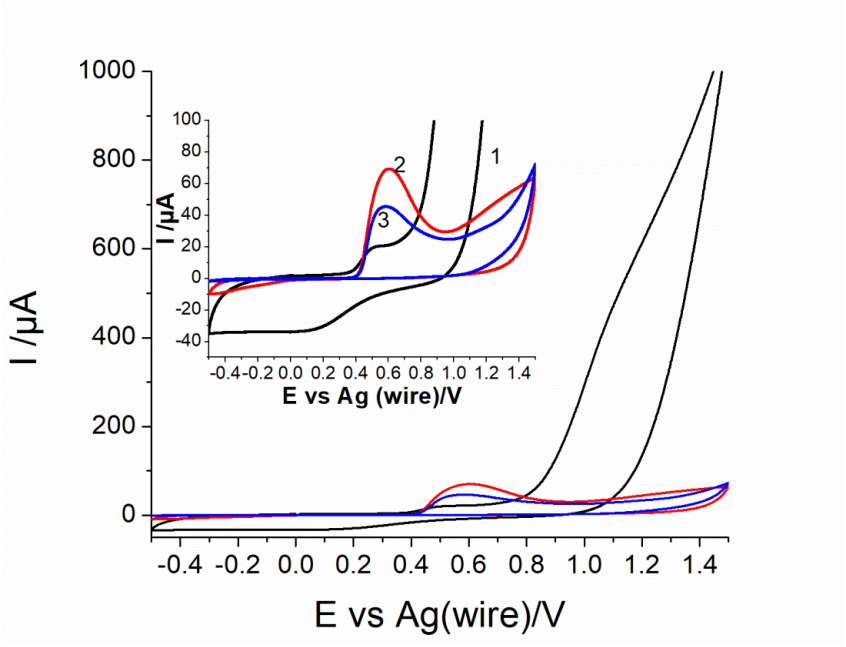

Figure S3: Study of potential interferences from the preservatives used in biopharmaceuticals containing sCT*:* Cyclic voltammograms of (1) salmon calcitonin (2 mg mL^{-1}); (2) m-cresol (0.13 mg mL^{-1}) and (3) phenol (1 mg mL^{-1}) in acetate buffer (0.1 M, pH 4.2) recorded with SPE-$(PDDA/prGO)_4$ electrodes, scan speed= 0.1V/s.

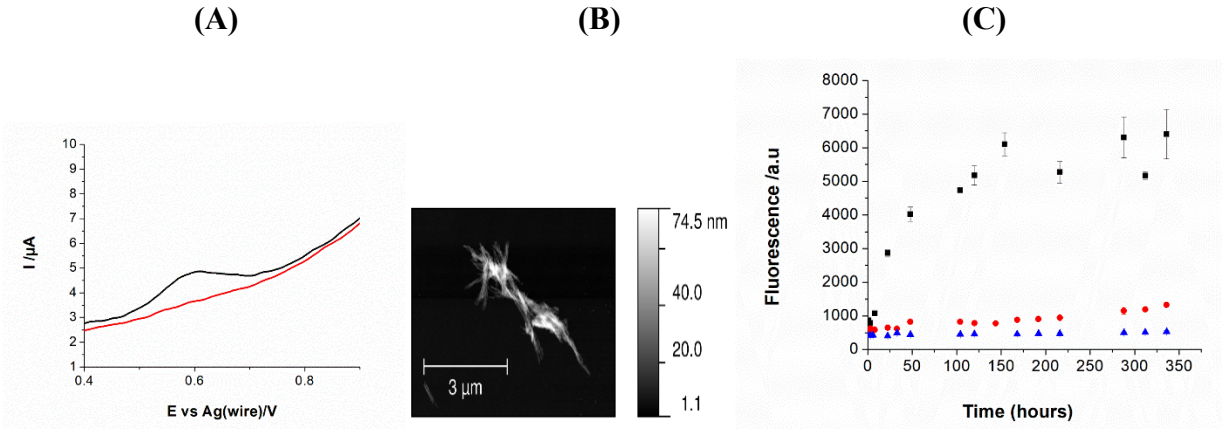

Figure S4. **Control experiments to prove that the electrochemical method is appropriate for the analysis of diluted sCT (8.35 µg mL^{-1}) undergoing amyloid type aggregation.** (A*)* SWV of a 8.35 µg mL^{-1} sCT in citrate buffer (10 mM, pH 6) freshly prepared (black) and after 14 days

at room temperature under shaking (red) recorded with SPE-$(PDDA/prGO)_4$. Conditions: potential step: 0.005 V, pulse amplitude: 0.04 V, scan between 0 and 1 V, frequency: 25 Hz; (B) AFM analysis of this solution after 14 days aggregation, (C) Measurements of the fluorescence of thioflavin T mixed with solutions of calcitonin 2 mg mL^{-1} (black squares), 50 µg mL^{-1} (red circles) and 8 µg mL^{-1} (blue triangles) in citrate buffer (10 mM, pH 6), submitted to aggregation at room temperature for different periods of time with (for 50 µg mL^{-1} and 8 µg mL^{-1}) or without stirring (2 mg mL^{-1}).